

Appearance of icosahedral atomic clusters in the formation of the MgCu₂-type structure from the bcc structure in Ti-Cr alloys

A. Hirata* and Y. Koyama

Kagami Memorial Laboratory for Materials Science and Technology, and Department of Materials Science and Engineering, Waseda University, Shinjuku-ku, Tokyo 169-0051, Japan

M. Tanimura

Research Department, Nissan ARC Ltd., 1 Natsushima-cho, Yokosuka, Kanagawa 237-0061, Japan

(Received 3 December 2002; published 29 April 2003)

The Cu₂Mg-type structure, called the C15 structure, is one of the covalency-involved structures in alloys and is characterized by a three-dimensional network of the covalent tetrahedra of small majority atoms. In order to understand the formation of covalent bonds in alloys, the crystallographic features of the C15 structure in the (bcc→hcp+C15) reaction of the Ti-(30- and 40-at. %) Cr alloys have been examined by transmission electron microscopy. It was found that the C15 structure was formed from the metallic bcc structure via the formation of icosahedral atomic clusters. Based on the shape of the icosahedral cluster, the cluster should be produced as a result of the local formation of covalent bonds along one of the $\langle 110 \rangle_B$ directions. It can thus be said that, in relation to the formation of the covalency-involved C15 structure from the metallic bcc structures, the local covalent bonds between two Cr atoms are first formed in the bcc matrix, and then that the local bonds are developed into the three-dimensional network of the covalent tetrahedra consisting of four Cr atoms.

DOI: 10.1103/PhysRevB.67.144107

PACS number(s): 61.66.Dk, 68.37.Lp

I. INTRODUCTION

It is known that the crystal structures of the Laves phases are characterized by an arrangement of complex coordination polyhedra.^{1,2} The Cu₂Mg-type structure called the C15 structure is one of such structures and consists of the 12- and 16-coordination polyhedra. Recently the tetrahedron of four small majority atoms in the 12-coordination polyhedron was found to involve a covalent nature of atomic bonds.^{3,4} It is thus understood that the C15 structure is one of covalency-involved structures in alloys. This gives us a motivation for investigating how a covalent bond is formed from a metallic structure in alloys. Among the Laves structures in alloys, in this work, we focus on the formation of the C15 structure from the bcc structure in the Ti-Cr alloys.

In the Ti-Cr alloy system, there exists the (bcc→hcp + C15) reaction in the composition range between 2-at. % Cr and 63-at. % Cr.⁵ We have already examined the crystallographic features of the reaction by transmission electron microscopy, using Ti-30-at. % Cr alloys.^{6,7} It was found that the reaction took place in the five steps; bcc→bcc+zone→bcc + CSS→bcc + CSS + hcp→bcc + hcp + C15→hcp + C15, where zone means a zone structure consisting of one Cr layer, and CSS denotes a chemical stripe structure characterized by three Ti layers and one Cr layer. The striking feature of the reaction to be noted here is that the precipitates developed into the C15-structure regions by the annealing were initially nucleated as a nm-size region. Electron diffraction patterns from the nm-size regions were, however, found to reveal only weak reflections. It is hard to explain these reflections as being due to the C15 structure. It can thus be said that both the structural model of the nm-size region and the formation path of the C15 structure from the bcc structure are still open to question. In this work, we have thus reex-

amined the crystallographic features of the covalency-involved C15 structure from the metallic bcc one by using Ti-30 and 40-at. % Cr alloys. Concretely, the Ti-30-at. % Cr alloy was mainly used to check the chronological evolution of the formation of the C15 structure. The crystallographic relationship between the bcc and C15 structures was, on the other hand, determined by using the Ti-40-at. % Cr alloy. This is because the annealing led to a larger size of the C15-structure region in the latter alloy, compared with the former. Based on the experimentally obtained data, further, we propose the formation model of the covalency-involved C15 structure from the metallic bcc structure in the Ti-Cr alloys.

II. EXPERIMENTAL PROCEDURE

Alloy samples of the Ti-30 and 40-at. % Cr alloys used in the present work were prepared according to the procedure described in our previous paper.⁶ In order to examine the formation path of the C15 structure from the bcc one, the alloy samples of a metastable bcc phase were annealed at 873 K for 3.5, 4, 5, and 100 h in the Ti-30-at. % Cr alloy, and for 1 and 5 h in the Ti-40-at. % Cr alloy, followed by quenching into ice water. Observation of the quenched samples was made at room temperature by using a JEM-3010 transmission electron microscope with an accelerating voltage of 300 kV. The crystallographic features of the formation of the C15 structure were examined by taking electron diffraction patterns, and bright and dark field images of each sample. Specimens for observation were prepared by an Ar-ion thinning technique.

Before presenting the experimental data obtained in this study, we briefly describe the characteristic features of both the C15 structure and a corresponding electron diffraction pattern in order to help the understanding of our experimental data. Figures 1(a) and 1(b) show the $[1\bar{1}0]$ projection of

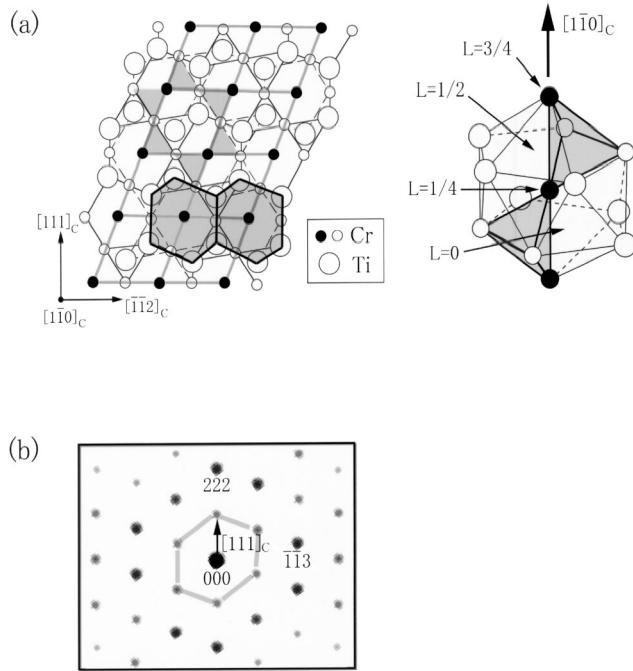


FIG. 1. (a) $[1\bar{1}0]_C$ projection of the C15 structure and (b) a corresponding calculated diffraction pattern. The 12-coordination polyhedron in the C15 structure is shown in the right side of (a).

the C15 structure and the $[1\bar{1}0]_C$ calculated diffraction pattern, respectively. Note that the subscript C denotes the C15 structure. The 12-coordination polyhedron in the C15 structure is also shown in the right side of (a). In the diagrams, the Cr and Ti atoms are represented by the small open and closed circles, and the large open circles, respectively. The striking feature is that the C15 structure can be regarded as a four-layer structure along the $[1\bar{1}0]_C$ direction. The four layers are specified as $L=0$, $\frac{1}{4}$, $\frac{1}{2}$, and $\frac{3}{4}$. When the atoms connected by thin dashed lines in the projection are assumed to be in the $L=0$ layer, those by solid lines sit on the $L=\frac{1}{2}$ layer. The 12-coordination polyhedron and the covalent tetrahedron involved in it are also shown by the gray regions of the distorted hexagonal and triangle shapes in the projection, respectively. In the three-dimensional diagram in the right side, further two tetrahedra connected each other are clearly seen in the 12-coordination polyhedron. It is thus understood that the C15 structure is characterized not only by the periodic arrangement of the 12-coordination polyhedra but also by the three-dimensional array of the tetrahedra with a covalent nature. That is, the C15 structure consists of the three-dimensional network of the covalent bond between two neighboring Cr atoms. The length of the covalent bond was estimated to be about 0.245 nm on the basis of the lattice constant already reported.⁸ It should be remarked that the 12-coordination polyhedron can be regarded as a distorted icosahedral atomic cluster.

The corresponding calculated diffraction pattern with the $[1\bar{1}0]_C$ incidence for the C15 structure is shown in Fig. 1(b). The pattern was actually calculated by assuming sample thickness of 10 nm. As is seen in the pattern, six diffraction

spots in smaller scattering angles are arranged in a distorted hexagonal shape around the origin 000, as indicated by the thick lines. It is here worth noticing that the $h00$ -type reflections with $h=4n-2$ are forbidden for the C15 structure. That is, the appearance of these reflections in the pattern is due to dynamical effect. In the case of sample thickness of more than 2 nm, anyhow, the $[1\bar{1}0]_C$ diffraction pattern of the C15 structure is characterized by these six reflections in the smaller-scattering-angle region, which are arranged with the distorted hexagonal shape. In keeping these features in mind, we have analyzed the orientation relationship between the bcc and C15 structures. In the pattern, the $[111]_C$ direction of the C15 structure is also represented by the arrow.

III. EXPERIMENTAL RESULTS

In the (bcc \rightarrow hcp + C15) reaction of the Ti-30-at. % Cr alloy, the precipitates developing into the C15 regions by the annealing were nucleated as a nm-size region around the hcp regions. The notable thing in the reaction is that the crystal structure of the nm-size region can not be identified as the C15 structure uniquely. That is, there is a possibility that the formation of the C15 structure is not simple but should involve a certain structural change. In this situation, we here start with the confirmation of these features and then describe the new experimental data obtained in this work.

A bright field image, a corresponding electron diffraction pattern, and a dark field image of the Ti-30-at. % Cr alloy annealed at 873 K for 3.5 h are, respectively, shown in Figs. 2(a), 2(b), and 2(c). The electron incidence of the images and the pattern is parallel to the $[110]_B$ direction, where the subscript B denotes the bcc structure. In the diffraction pattern, there are three types of the reflections indicated by the arrows A, B, and C, in relation to the presence of the bcc matrix, the hcp precipitates, and the nm-size regions in the sample. The strong reflections A are due to the bcc matrix, while the hcp precipitates give rise to the reflections B observed as a very sharp spot. Based on the locations of these reflections in the pattern, the orientation relationship between the bcc and hcp structures was confirmed to be the Burger's relation of $(110)_B \parallel (00 \cdot 1)_H$ and $[112]_B \parallel [10 \cdot 0]_H$. Note that the subscript H means the hcp structure. In addition to these reflections, the weak reflections C are present in the pattern. The notable feature of the weak reflections is that ten diffraction spots with relatively wide intensity distribution are arranged with a pseudodecagonal shape, as indicated by ten thick and short arrows. As was mentioned earlier, the weak reflections can not, however, be explained as being due to the C15 structure. Then we took dark field images by using these reflections. As a result, two kinds of regions in the bright field image, which are, for instance, marked by A and B, were confirmed to have the bcc and hcp structures, respectively. Many nm-size regions were, on the other hand, observed in images for the weak reflection. Figure 2(c) is one of dark field images showing the nm-size regions, which were taken by the weak reflection indicated by the arrow C. We can clearly see the regions with an average size of about 2 nm in the image. Note that these regions were developed into the C15 regions in the subsequent annealing. It is further

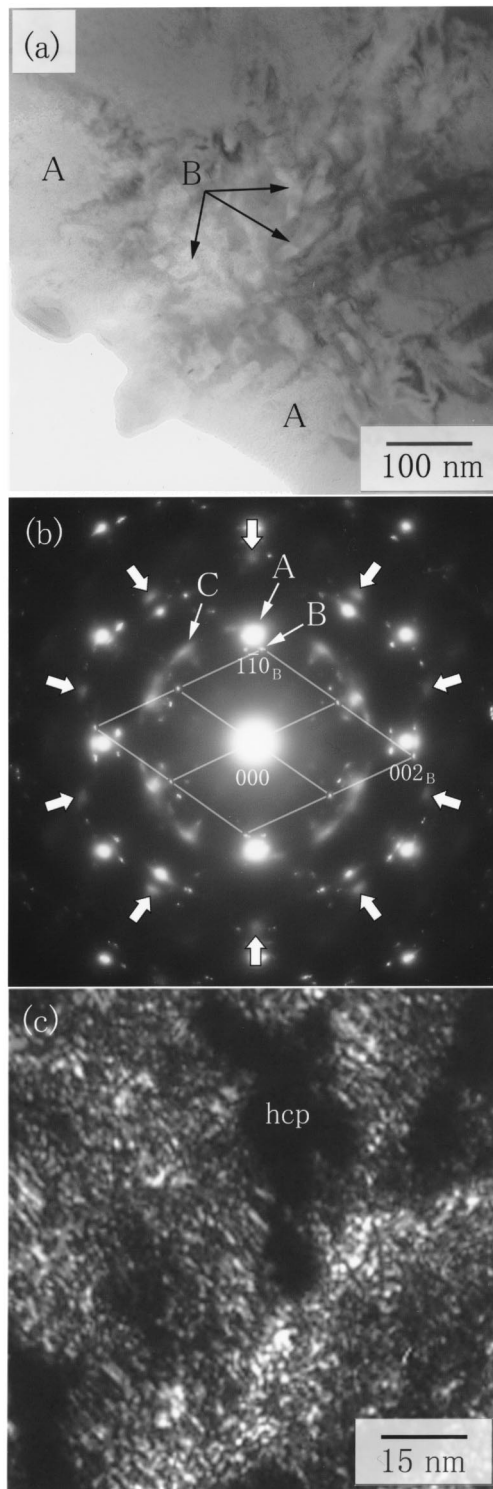


FIG. 2. (a) Bright field image, (b) a corresponding electron diffraction pattern, and (c) a dark field image obtained from the Ti-30-at. % Cr alloy sample annealed at 873 K for 3.5 h.

worth noting that diffraction patterns with the other $\langle 110 \rangle_B$ incidences basically exhibit the same features as the pattern in Fig. 2(b).

A change in the diffraction pattern in the annealing after the appearance of the nm-size region is shown in Fig. 3.

Figures 3(a), 3(b), and 3(c) are, respectively, $[110]_B$ diffraction patterns of the Ti-30-at. % Cr alloy samples annealed for 3.5, 4, and 5 h. The pattern in Fig. 3(a) is the same as that in Fig. 2(b), and the inset of Fig. 3(c) is an enlarged pattern of Fig. 3(c) in the smaller-scattering-angle region. When the sample was kept at 873 K, the intensities of the weak reflections increase first, but the hcp reflections become rather diffuse, as is indicated by the arrow A. The spread of the intensity distribution for the hcp reflection implies that the hcp regions are reduced in size. In addition, the appearance of the weak reflections in the smaller-scattering-angle region can be detected, as shown by the arrow B in Fig. 3(b), in spite of their very diffuse intensity distribution. On further annealing, the hcp and weak reflections become sharp, as is shown in Fig. 3(c). The important feature is that the distorted hexagonal arrangement of six weak reflections, indicating the presence of the C15 structure, is clearly seen in the smaller-scattering-angle region, as shown in the inset of Fig. 3(c). In fact, the weak reflections in this region indicate that there are some variants of the C15 structure. On the other hand, the bcc reflections are still present in the 5-h annealing, as is indicated by the arrow C. It is thus understood that there coexist bcc-, hcp-, and C15-structure regions in the 5-h annealing sample.

A bright field image of the 30-at. % Cr alloy sample annealed for 100 h is shown in Fig. 4(a), together with a corresponding electron diffraction pattern in Fig. 4(b). Note that the 100-h annealing sample already reached the equilibrium (hcp+C15) state. In the pattern, there are relatively sharp reflections due to both the hcp and C15 structures. But the bcc reflection cannot be detected in the pattern, as is shown by the arrow. It is then understood that the characteristic features of the diffraction pattern in Fig. 4(a) are basically the same as those in Fig. 3(c), except for the missing of the bcc reflection. That is, the pattern should correspond to the $[110]_B$ pattern with no bcc reflection. In addition, selected-area patterns taken by using a smallest-size aperture revealed that the regions marked by A and B in the image correspond to those of the hcp and C15 structures, respectively. An average size of the hcp and C15 regions was determined to be about 100 nm.

As was mentioned above, the distorted hexagonal arrangement of the six reflections in the smaller-scattering-angle region was detected in the $[110]_B$ diffraction patterns of the bcc structure. This implies that the C15 region has the specific orientation relationship to the bcc matrix; that is, $[110]_B \parallel [1\bar{1}0]_C$. This relation is here referred to as the first condition. Because the C15 regions in the Ti-40-at. % Cr alloy can grow faster and larger than those in the Ti-30-at. % Cr, it is easy to determine the second condition between the bcc and C15 structures by using the 40-at. % Cr alloy. It was, as a result, found that in the case of $[110]_B \parallel [1\bar{1}0]_C$ there are seven relations as the second condition with respect to the angle θ between the $[1\bar{1}0]_B$ direction in the bcc structure and the $[111]_C$ direction in the C15 structure. Seven electron diffraction patterns indicating these seven relations between the bcc and C15 structures are shown in Fig. 5, together with a schematic diagram showing the angles for the relations.

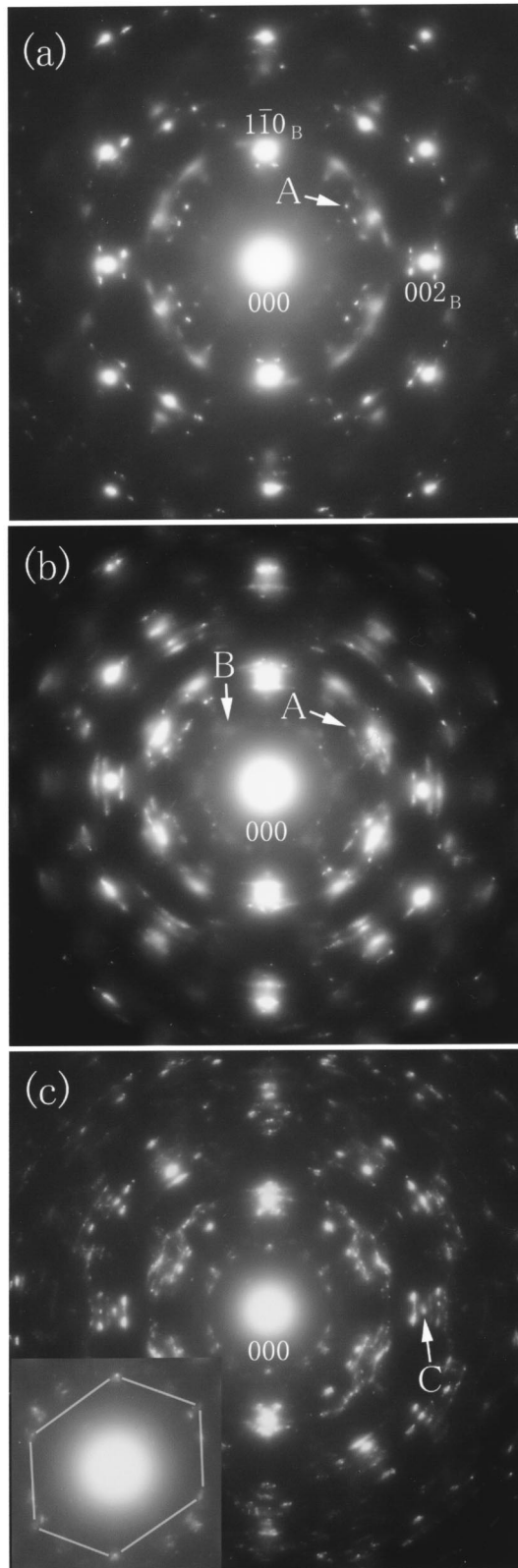


FIG. 3. A series of electron diffraction patterns taken from the Ti-30-at.% Cr alloy samples annealed for (a) 3.5 h, (b) 4 h, and (c) 5 h. An enlarged pattern of (c) is shown in the inset.

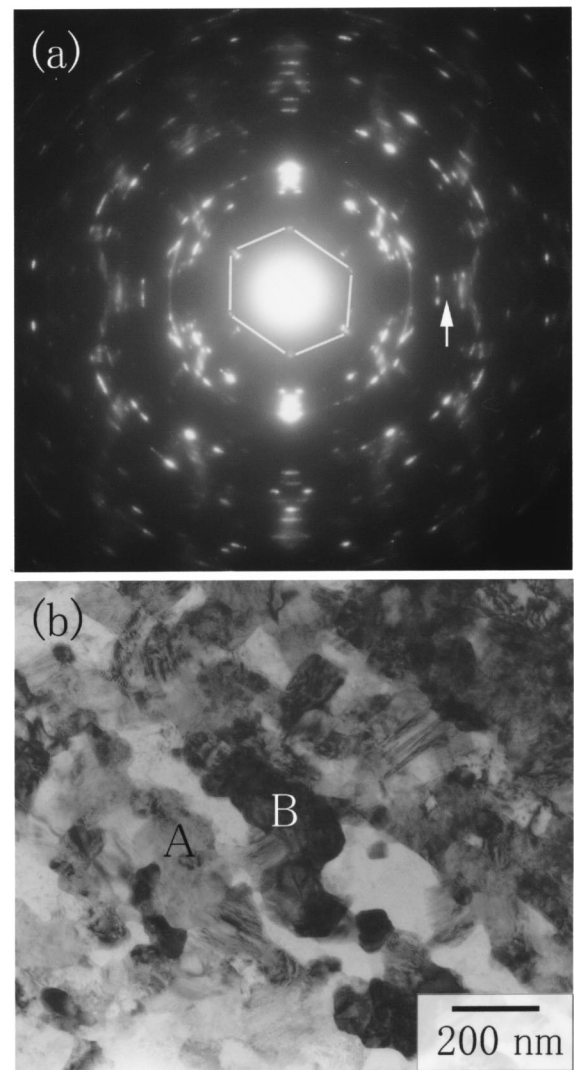


FIG. 4. (a) Electron diffraction pattern and (b) a bright field image taken from the 30-at.% Cr alloy sample annealed for 100 h.

These patterns were taken from the Ti-40-at.% Cr alloy annealed for 1 h and the electron incidence of all patterns is parallel to the $[110]_B$ direction; that is, the $[1\bar{1}0]_C$ direction. In each pattern, the $[111]_C$ direction in the C15 structure is represented by the arrow, just like Fig. 1(b). We can clearly see the distorted-hexagonal arrangement of the six C15 reflections in the smaller-scattering-angle region of each pattern, as indicated by the white lines, in addition to the bcc reflections. The angles of the seven relations for the second condition were found to be $\theta=0^\circ, 30^\circ, 38^\circ, 72^\circ, 80^\circ, 108^\circ,$ and 144° . It is obvious that these angles should be a key factor to understand the formation of the C15 structure from the bcc one. Based on these angles, we actually tried to construct a model for the formation of the C15 structure. It is further understood that, when the other $\langle 110 \rangle_B$ directions are taken into account for the first condition, $84 (=7 \times 12)$ variants of the C15 structure are possible in the formation of the C15 structure in the Ti-Cr alloys.

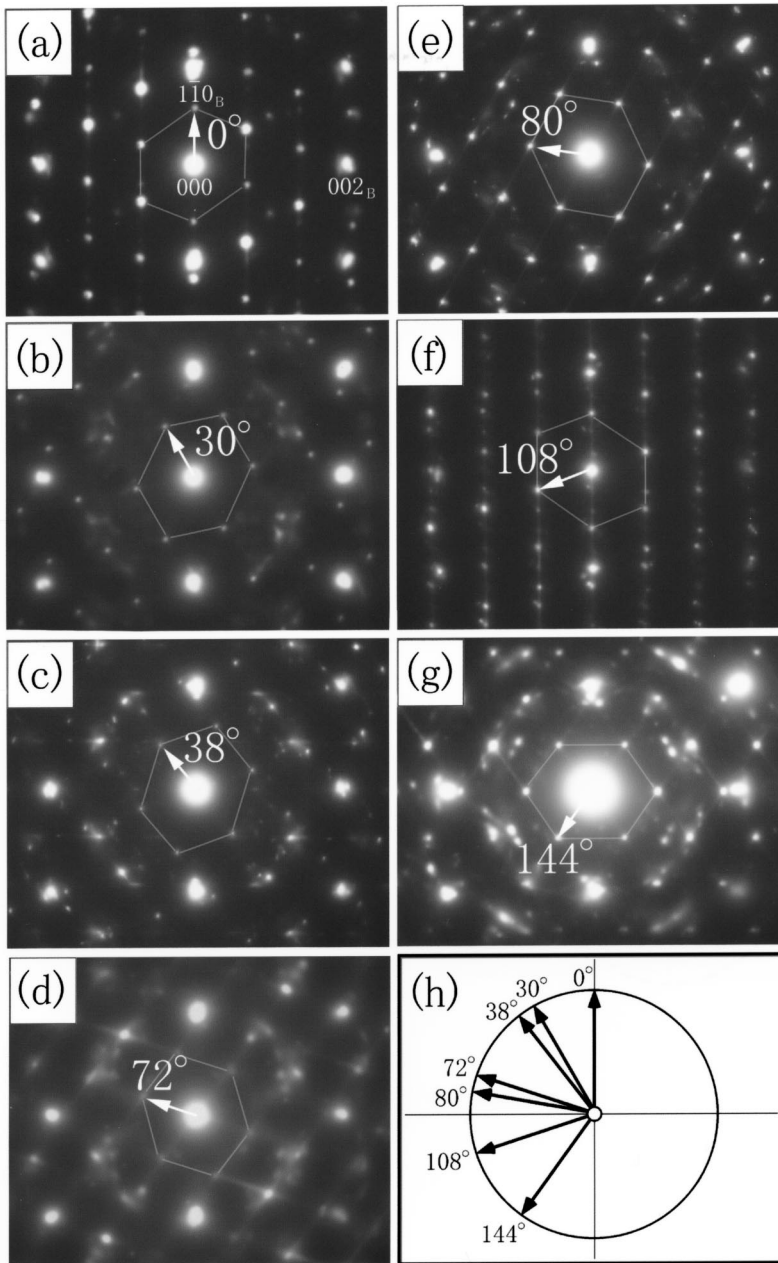


FIG. 5. Electron diffraction patterns showing the presence of seven C15 variants, obtained from the Ti-40-at. % Cr alloy sample annealed for 1 h at 873 K. The angle θ between the $[1\bar{1}0]_B$ direction in the bcc structure and the $[111]_C$ direction in the C15 structure for the seven variants is schematically shown in (h).

IV. DISCUSSION

The present experimental data revealed that, although the crystal structure of the nm-size region developing into the C15 region could not be identified uniquely, the C15 region had the specific relationship to the bcc matrix. The most striking feature is that, in the case of the relation of $[110]_B \parallel [1\bar{1}0]_C$ for the first condition, there are the seven relations between the $[1\bar{1}0]_B$ direction in the bcc structure and the $[111]_C$ direction in the C15 structure for the second condition. This suggests that some structural change should be involved in the formation of the covalent-involved C15 structure from the metallic bcc one in the Ti-Cr alloys. Here, we first show the structural correspondence between the bcc and C15 structures on the basis of the seven angles for the second condition. An appropriate model for the formation of

the C15 structure from the bcc one is also proposed in relation to the formation of the covalent bond in alloys.

The structural correspondence between the bcc and C15 structures based on the orientational relationship obtained in the work is shown here. In the case of $[110]_B \parallel [1\bar{1}0]_C$ for the first condition, there exist the seven relations between the $[1\bar{1}0]_B$ and $[111]_C$ directions for the second condition. These seven relations can be specified by using the angle θ between the $[1\bar{1}0]_B$ and $[111]_C$ directions. As is shown in Fig. 5, the value of θ was found to be $\theta = 0^\circ, 30^\circ, 38^\circ, 72^\circ, 80^\circ, 108^\circ,$ and 144° . The $[110]_B$ structural projections of the C15 variants for these seven θ values with respect to the original bcc orientation are depicted in Fig. 6. The gray triangles in each projection represent the covalent tetrahedra consisting of four small majority atoms. As is understood in

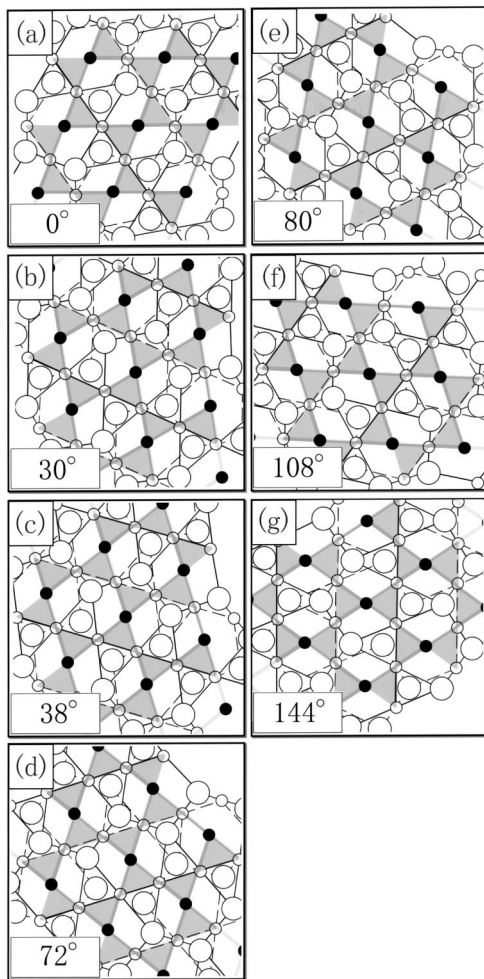


FIG. 6. $[110]_B$ structural projections of seven C15 variants derived from the obtained orientation relationship.

these diagrams, the array of the tetrahedra is rotated, corresponding to the value of θ . This gives us the simple question why the array of the tetrahedra is rotated. In order to answer this question, we propose a model for the formation of the C15 structure from the bcc structure in the Ti-Cr alloys.

As was shown in Fig. 6, there exist the seven relations between the bcc and C15 structures for the second condition. This fact seems to imply that the formation of the covalency-involved C15 structure from the metallic bcc structure is not simple but involves some structural change. In the present work, in fact, the crystal structure of the nm-size region developed into the C15 region by the annealing could not be determined uniquely. In addition, the other crucial features to be noted are that the pseudo decagonal arrangement of the weak reflections was observed in the diffraction pattern of the 3.5-h annealing sample, and that all $\langle 110 \rangle_B$ diffraction patterns basically exhibit the same features as for the weak reflections. Based on these features, we here propose the formation model of the C15 structure from the bcc one, as is shown in Fig. 7. The striking feature of the model is that the C15 structure is assumed to be formed from the bcc structure via the formation of the icosahedral atomic cluster. The formation of the icosahedral atomic cluster from the bcc struc-

ture is depicted in Fig. 7(a), together with the structural change from the cluster to the seven C15 variants in Fig. 7(b). As is understood in Fig. 7(a), the icosahedral atomic cluster can be obtained from the bcc structure by simple atomic shifts. When the $[110]_B$ direction in the bcc structure is assumed to be the L axis, the atoms in the bcc structure originally sit only on the $L=0$ and $\frac{1}{2}$ layers, but two atoms around the center of the projection move to the positions of the gray atoms in the $L=\frac{1}{4}$ or $\frac{3}{4}$ layer of the cluster. That is, the shifts of the gray atoms in the formation of the cluster involve the component along the $[110]_B$ direction. The second step shown in Fig. 7(b) obviously takes place in order to form the C15 structure having the covalent tetrahedra from the icosahedral atomic cluster. It is concretely assumed that the decagonal column is first formed by connecting some icosahedral atomic clusters along the $[110]_B$ direction, and that the decagonal columns are then connected to one another. In the connection, the flat boundary between two neighboring columns, indicated by the thick lines in Fig. 7(b), is formed by simple atomic shifts. Based on this scenario, we tried to find possible variants of the C15 structure. Under the assumption that each icosahedral cluster in the decagonal column should be formed from the bcc structure in the way shown in Fig. 7(a), it was found that, in the case of the connection of four decagonal columns, there are seven possible variants in Fig. 7(b). The angles θ for these seven variants were determined to be $\theta=0^\circ, 30^\circ, 38^\circ, 72^\circ, 80^\circ, 108^\circ,$ and 144° . That is, the values of the angles are exactly the same as those obtained experimentally. We believe that this agreement guarantees the validity of our model. As is understood in Fig. 7(b), a further characteristic feature of these C15 variants is that the formation of the covalent tetrahedra shown by the gray triangles in Fig. 7(b) is directly associated with the formation of the flat boundary between two neighboring columns. It is eventually understood that the selection of a variant among the seven possible C15 variants depends on how the decagonal columns are connected one another.

As was mentioned just above, the C15 structure is formed from the bcc structure via the icosahedral atomic cluster in our model. In order to get direct evidence of the presence of the icosahedral atomic cluster, we took electron diffraction patterns of the nm-size regions in the 3.5-h annealing sample of the Ti-30-at. % Cr alloy. Figure 8 shows a series of six diffraction patterns of the 3.5-h annealing sample, together with the stereographic projection of icosahedral symmetry. These patterns were taken by rotating the sample about the $[1\bar{1}0]_B$ direction from the $[110]_B$ incidence. The electron incidence of each pattern is specified not only in the bcc notation but also by using the angle α between the incidence and the $[110]_B$ direction. Although there are the bcc and hcp reflections and some weak reflections due to the icosahedral clusters overlap the bcc reflections, the pseudo-fivefold, -threefold, and -twofold patterns for the weak reflections, as indicated by the arrows in these patterns, are actually obtained near the incidences expected from the stereographic projection. The slight difference between the expected and experimental angles should be due to both the experimental error concerning the measurement of the rotation angle and

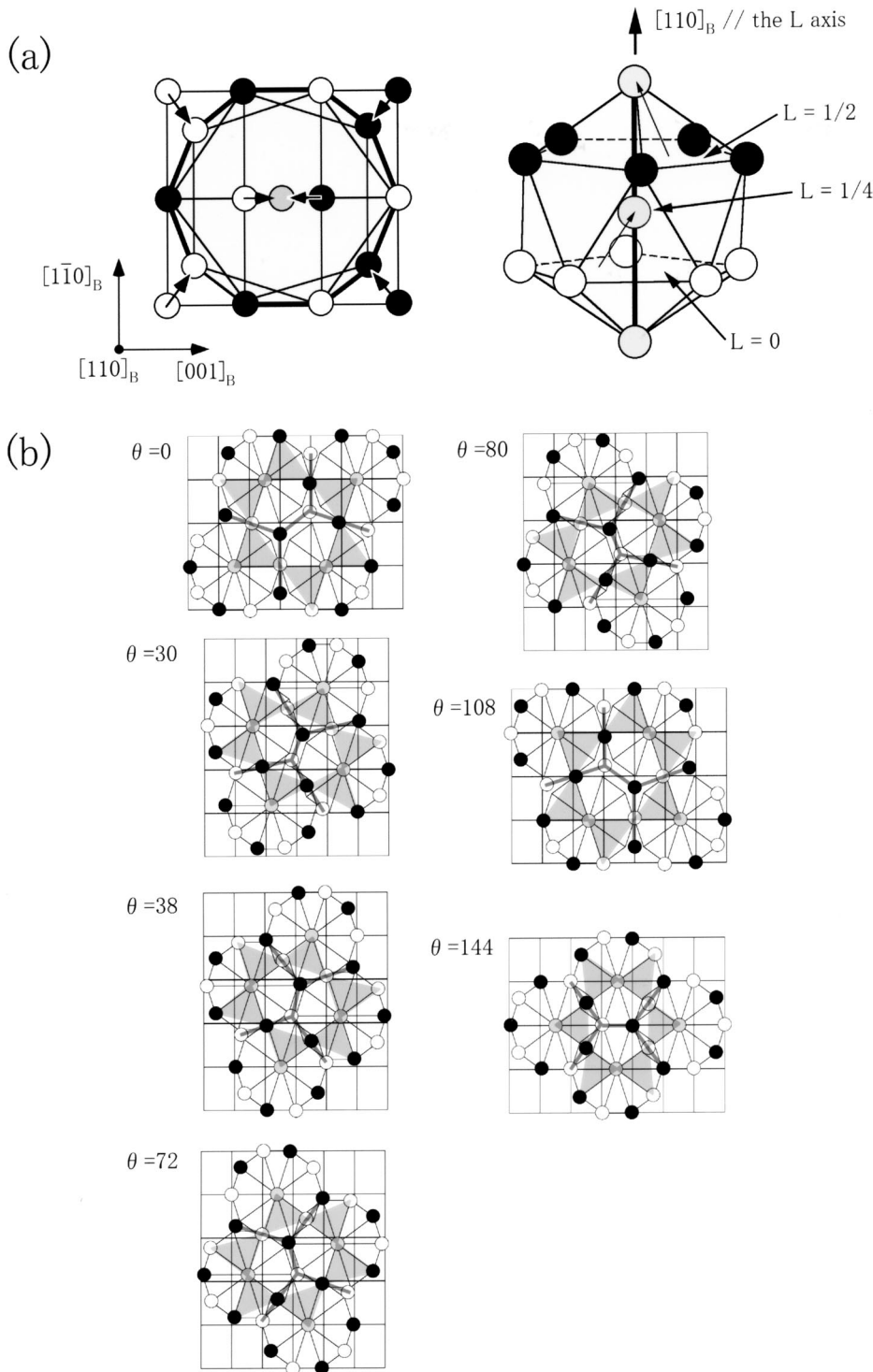


FIG. 7. (a) Schematic diagram showing the formation of the icosahedral atomic cluster from the bcc structure, together with (b) seven C15 variants predicted in our model. The three-dimensional diagram of the icosahedral atomic cluster is shown in the right side of (a).

the spatial spread of the weak reflections in reciprocal space. It is obvious that the spatial spread is ascribed to a small size of the nm-size region. We thus believe that based on these diffraction patterns the icosahedral atomic clusters really appear in the formation of the C15 structure from the bcc structure in the Ti-Cr alloys.

We here check the shape of the icosahedral atomic cluster appearing in the formation of the C15 structure from the bcc structure. In order to do this, we pay attention to the diffrac-

tion pattern with $\alpha = +65^\circ$ in Fig. 8. This is because in this pattern the arrangement of the ten diffraction spots characterizing the presence of the cluster reflects its sizes along the $[110]_B$ direction as well as along the direction perpendicular to it. Figure 9 is a $[113]_B$ nanobeam electron diffraction pattern with $\alpha = +65^\circ$ of the 30-at% Cr alloy sample annealed for 3.5 h, which was taken from an area consisting of nm-size regions. A size of the area was estimated to be about 20 nm. In the pattern, ten diffraction spots are clearly seen,

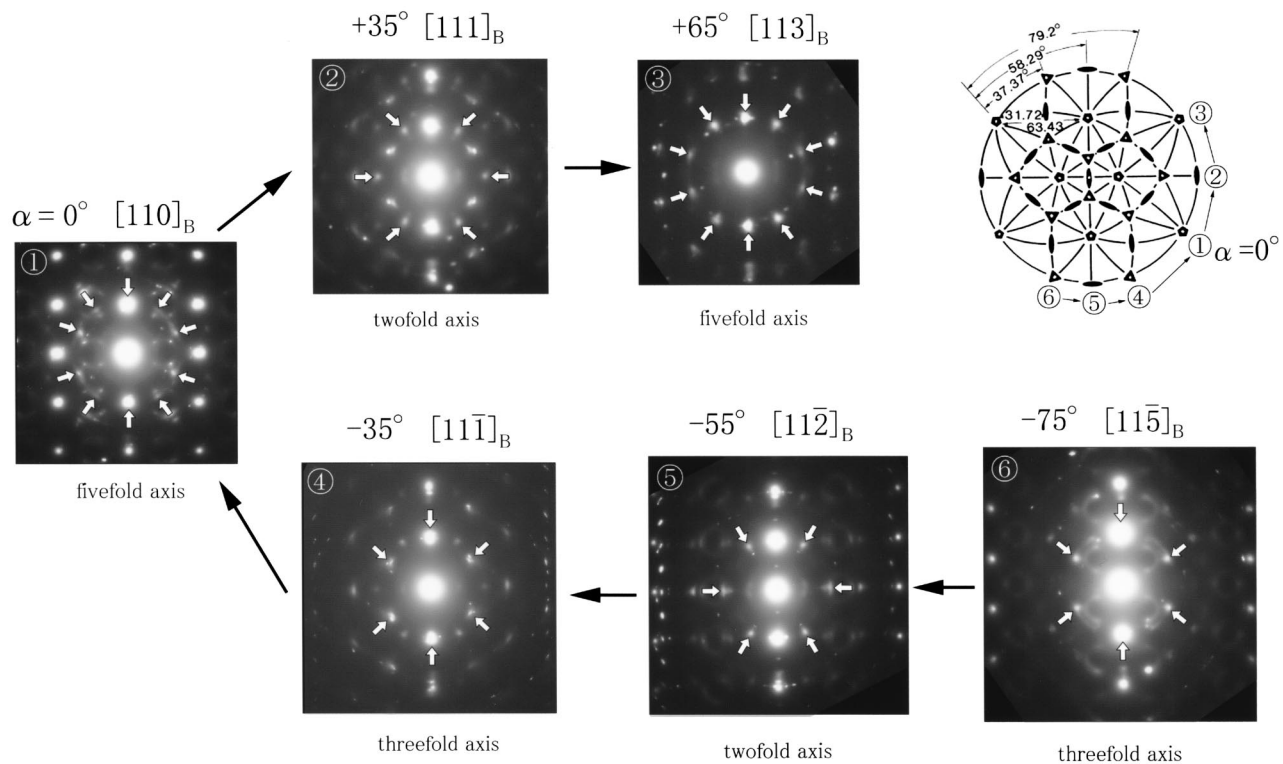


FIG. 8. A series of six diffraction patterns of the 3.5-h annealing sample of the Ti-30-at. % Cr alloy, together with the stereographic projection of icosahedron symmetry.

although two of them overlap the $1\bar{1}0_B$ and $\bar{1}10_B$ reflections due to the bcc structure. The interesting feature is that the arrangement of these ten spots is slightly distorted from the ideal decagonal shape. In the pattern, concretely, the length A is slightly shorter than the length B . This implies that the icosahedral cluster should be compressed along the $[110]_B$ direction. In other words, the shortest bonds are formed in the icosahedral cluster along the $[110]_B$ direction, as indicated by the thick lines in the lower side of Fig. 9. Because the length of the shortest bond is estimated to be about 0.238 nm, it is suggested that the formation of the icosahedral cluster is ascribed to that of the local covalent bonds along the $[110]_B$ direction. Note that the covalent tetrahedron of the C15 structure in the Ti-Cr alloys was reported to have the bond length of 0.245 nm, as mentioned earlier.

The nm-size regions are understood to consist of the icosahedral atomic cluster. This indicates that there coexisted the nm-size, icosahedral-cluster region, the hcp precipitates, and the bcc matrix in the Ti-30-at. % Cr alloy annealed for 3.5 h, as is shown in Fig. 2. As a matter of fact, the icosahedral-cluster regions were formed in Cr-rich areas of the bcc matrix, which were produced by the appearance of the hcp precipitates as the equilibrium phase in the Ti-rich side. In this state, the hcp precipitates and the bcc matrix satisfy the Burger's relation as the crystallographic orientation relationship, and the icosahedral cluster has the specific relation to the bcc matrix, as is shown in Fig. 7(a). As a result, a unique relation exists between the icosahedral cluster and the hcp precipitate, too. In the case of the hcp variant with the relation of $[110]_B \parallel [00 \cdot 1]_H$, for instance, the clus-

ter axis of the icosahedral cluster should be parallel to the $[00 \cdot 1]_H$ direction of the hcp variant.

When the Ti-30-at. % Cr alloy was further annealed from the state mentioned just above, the icosahedral-cluster regions became the C15 variants, together with the increase in the size of the regions. The thing to be noted here is that, as is shown in Fig. 7(b), the C15 variants basically have the specific orientation relationship with the bcc matrix. Although the size of the hcp precipitates was first reduced, the growth of them also occurred, keeping the orientation relationship with the bcc matrix. These are based on the fact that the C15 and hcp reflections are basically observed as the rather spotty shape in Fig. 3(c), although the non-radial, weak intensity distribution can be detected around some spotty reflections. In the diffraction pattern of the 100-h annealing sample in Fig. 4, on the other hand, we clearly see the non-radial intensity distribution indicating the slight lattice rotation. The simple analysis of the pattern showed that the lattice rotation occurred mainly for the C15 variants, except for the C15 variants with the relation of $[110]_B \parallel [1\bar{1}0]_C$. In addition, the degree of the lattice rotation in the Ti-30-at. % Cr alloy was found to be more conspicuous than that in the Ti-40-at. % Cr alloy. It seems to us that the lattice rotation results from the annihilation of the bcc matrix, and that the difference in the degree is due to the volume fraction of the hcp precipitates to the C15 variants.

It is time to discuss the physics of the formation of the C15 structure from the bcc structure in relation to the formation of the covalent bonds in alloys. As was mentioned earlier, the tetrahedron of the small majority Cr atoms in the

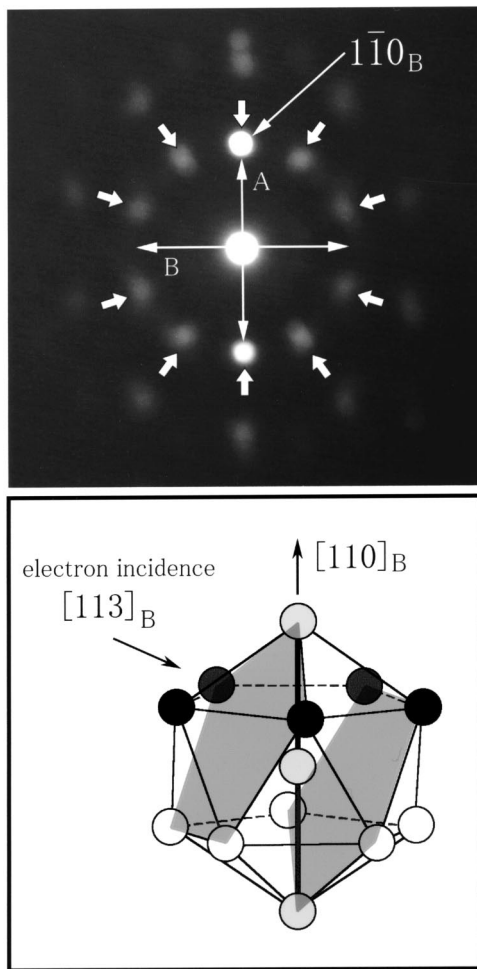


FIG. 9. Nano beam electron diffraction pattern with the $[113]_B$ incidence of $\alpha = +65^\circ$ from nm-size regions in the 30-at.% Cr alloy sample annealed for 3.5 h. The schematic diagram of the icosahedral cluster is also depicted to show the direction of the $[113]_B$ electron incidence against the icosahedral cluster.

12-coordination polyhedron has a covalent nature. This was also confirmed by our cluster calculation for a 12-coordination polyhedron, using the $DV-X\alpha$ technique. The C15 structure is thus characterized by the three-dimensional network of the covalent bonds between two neighboring Cr atoms. In other words, the formation of the C15 structure from the bcc structure reflects the development of the three-dimensional network of the covalent bonds. In this background, the present study revealed that the C15 structure was

formed from the bcc structure via the formation of the icosahedral atomic cluster. The notable feature of the icosahedral cluster is that the cluster has the covalent bonds along the cluster axis parallel to the $[110]_B$ direction in the case of Fig. 7(a). Because the covalent bond is formed between two neighboring Cr atoms, the appearance of the icosahedron cluster results from the local formation of the covalent Cr bonds along the cluster axis. In the annealing of the sample, the local covalent bond in the icosahedral cluster must be extended along the cluster axis. The extension of the covalent bonds results in the formation of the decagonal column. That is, the one-dimensional covalent chain must be formed along the centerline of the decagonal column. When the sample is further annealed, the decagonal columns appear in neighbors and contact one another. As a result of the contact, the flat boundary between two neighboring columns is formed by simple atomic shifts, as shown in Fig. 7(b). The important features are that the shifts occur only in the surrounding atoms around the centerline of the column, and that the shifts result in the formation of the covalent tetrahedron; that is, the unit of the three-dimensional network of the covalent bonds. The three-dimensional network of the covalent bonds in the C15 structure is then developed by both the further extension of the covalent chain along the centerline of the column and the further contact of the columns with other columns. It is eventually understood that the changes from the icosahedral cluster to the decagonal column and then to the C15 structure present the formation path of the three-dimensional network of the covalent bonds in the Ti-Cr alloys.

V. CONCLUSION

Based on the present experimental data, the formation of the C15 structure in the $(bcc \rightarrow hcp + C15)$ reaction by the annealing was understood to occur in two steps. The first step is the formation of the icosahedral atomic cluster from the bcc structure. The second step is associated with the formation of the C15 variants from the icosahedral cluster. Because the Cr tetrahedron in the 12-coordination polyhedron of the C15 structure has a covalent nature, the formation of the C15 variants reflects the development of the three-dimensional covalent network. Concretely the local covalent bonds characterizing the icosahedral cluster are first formed along one of the $\langle 110 \rangle_B$ directions. The three-dimensional network of the covalent bonds then results from both the extension of the local covalent bonds into the covalent chain characterizing the decagonal column and the formation of the covalent tetrahedra by the simple atomic shifts of the surrounding atoms in the decagonal column.

*Present address: The Institute of Scientific and Industrial Research, Osaka University, Ibaraki, Osaka 567-0047, Japan.

¹F. C. Frank and J. S. Kasper, *Acta Crystallogr.* **11**, 184 (1958).

²F. C. Frank and J. S. Kasper, *Acta Crystallogr.* **12**, 483 (1959).

³Y. Kubota, M. Takata, M. Sakata, T. Ohba, K. Kifune, and T. Tadaki, *J. Phys.: Condens. Matter* **12**, 1253 (2000).

⁴Y. Kubota, M. Takata, M. Sakata, T. Ohba, K. Kifune, and T. Tadaki, *Jpn. J. Appl. Phys., Suppl.* **38-1**, 456 (1999).

⁵J. L. Murray, *Bull. Alloy Phase Diagrams* **2**, 174 (1981).

⁶A. Hirata, M. Tanimura, and Y. Koyama, *Mater. Trans., JIM* **42**, 2553 (2001).

⁷A. Hirata, M. Tanimura, and Y. Koyama, *Mater. Trans., JIM* **43**, 1689 (2002).

⁸K. C. Chen, S. M. Allen, and J. D. Livingston, *J. Mater. Res.* **12**, 1472 (1997).